Journal of Cleaner Production 316 (2021) 128274

Contents lists available at ScienceDirect

Journal of Cleaner Production

journal homepage: www.elsevier.com/locate/jclepro

Spatially explicit changes in forest biomass carbon of China over the past 4 decades: Coupling long-term inventory and remote sensing data

Miaomiao Zhao [a,b], Jilin Yang [c,b,*], Na Zhao [a,b], Luo Liu [d], Ling DU [e], Xiangming Xiao [e], Tianxiang Yue [a,b,**], John P. Wilson [a,b,f]

[a] State Key Laboratory of Resources and Environmental Information System, Institute of Geographic Sciences and Natural Resources Research, Chinese Academy of Sciences, Beijing, 100101, China
[b] University of Chinese Academy of Sciences, Beijing, 100049, China
[c] Key Laboratory of Land Surface Pattern and Simulation, Institute of Geographic Sciences and Natural Resources Research, Chinese Academy of Sciences, Beijing, 100101, China
[d] Guangdong Province Engineering Research Center for Land Information Technology, The College of Natural Resources and Environment, South China Agricultural University, Guangzhou, 510642, China
[e] Department of Microbiology and Plant Biology, Center for Spatial Analysis, University of Oklahoma, Norman, OK, 73019, USA
[f] Spatial Sciences Institute, University of Southern California, Los Angeles, CA, 90089, USA

ARTICLE INFO

Handling editor: Bin Chen

Keywords:
China
Forest biomass
Carbon sinks
Forest inventories
Forest cover distribution

ABSTRACT

Quantification of the spatial pattern of forest carbon (C) sinks in high resolution is helpful to reveal the factors that affect the C cycle and provides valuable information for developing sustainable forest management policies. Here we developed a method using the data of long-term forest inventories (1977–2018) and spatially-explicit remotely sensed information from land-use maps and the Normalized Difference Vegetation Index (NDVI) datasets, to estimate the spatial and temporal variation of forest biomass C in China. At first, we calculated forest biomass C stocks using the refined Continuous Biomass Expansion Factor (CBEF) model with parameters for each forest type based on eight national forest inventories. Secondly, based on multi-temporal land-use remote sensing and national forest inventory datasets, we obtained forest coverage datasets with high resolution (1 km*1 km). Thirdly, we downscaled the forest biomass C density using the calibrated forest coverage maps and the maximum NDVI values derived from GIMMS-NDVI3g imagery. Our results showed that China's forest functioned as a C sink of 3777.73 Tg C, and the C density of forest stands increased from 35.41 Mg C ha^{-1} during 1977–1981 to 43.95 Mg C ha^{-1} during 2014–2018. In addition, the validation results for most of the provinces based on published inventory estimates during the eight periods showed that the forest area at the pixel scale was successfully calibrated. From this, we produced the maps with a finer resolution for a series of spatially continuous forest biomass carbon density distribution and carbon sinks. Notably eight major forest projects have accounted for 44%–51% of the forest C stocks added in China from 1977 to 2018. Our research provides new insights for understanding and monitoring the spatiotemporal variations in of forest biomass and key information to support the development of new afforestation policies moving forward.

1. Introduction

Forests are one of the important terrestrial ecosystems and play a prominent role in the global carbon (C) cycle, incorporating about 80% of the aboveground biomass C and 40% of below ground C in terrestrial ecosystems (Dixon et al., 1994; Bonan et al., 2008; Arneth et al., 2010; Pan et al., 2011; Qin et al., 2019). Accurate estimation of the spatial and temporal variation in forest C sinks can help to: (1) identify the factors driving C cycling; (2) predict the future changes in forest C sinks; and (3) provide a baseline for verifying the simulation results of ecosystem

* Corresponding author. Key Laboratory of Land Surface Pattern and Simulation, Institute of Geographic Sciences and Natural Resources Research, Chinese Academy of Sciences, Beijing, 100101, China.
** Corresponding author. State Key Laboratory of Resources and Environmental Information System, Institute of Geographic Sciences and Natural Resources Research, Chinese Academy of Sciences, Beijing, 100101, China.
E-mail addresses: yangjl.17b@igsnrr.ac.cn (J. Yang), yue@lreis.ac.cn (T. Yue).

https://doi.org/10.1016/j.jclepro.2021.128274
Received 1 February 2021; Received in revised form 7 July 2021; Accepted 9 July 2021
Available online 10 July 2021
0959-6526/

process models (Fang et al., 2001, 2018; Ju et al., 2007). In previous studies, regional forest biomass estimation relied on forest inventory statistics and lacked fine-scale spatial information, or the spatial pattern was presented notwithstanding large uncertainties due to the lack of field sample data and fine-resolution remotely sensed data (Fang et al., 2007; Piao et al., 2005, 2009; Gong et al., 2012; Zhang et al., 2013, 2015; Chen et al., 2019).

Characterizing the spatiotemporal variation of forest C sinks in China is necessary to understand forest ecosystem C dynamics and to quantify the contributions of reforestation and afforestation to C sequestration in past decades and better stewardship of the forests in the future (Chen and Luo, 2015; Babcock et al., 2016; Matasci et al., 2018). Generally, forest inventories are recognized as the most accurate method to assess forest biomass and C density at regional scales. China has conducted 5-year national forest inventories since the 1970s (Fang et al., 2001, 2007; Pan et al., 2004, 2011; Zhang et al., 2013, 2015) and the method based on the allometric relationships between forest biomass and timber volume proposed by Fang et al. (2001) has been widely used to estimate forest carbon stocks (e.g. Fang et al., 2007, 2014; Pan et al., 2011; Zhang et al., 2015). However, inventory data cannot document the continuous spatial patterns of forest C sinks at large scales (Brown, 2002; He et al., 2017). Remote sensing makes up for this deficiency and enables the estimation of forest biomass at multiple scales with large spatial and temporal coverage (Gong et al., 2012). The description of the relationships between biomass and the Normalized Difference Vegetation Index (NDVI) or Net Primary Production (NPP) remote sensing products is challenging due to the complexities of the canopy characteristics and limitations of using radar and Light Detection and Ranging (LiDAR) data in large scale studies because of expensive cost (Rauste, 2005; Piao et al., 2005; Kindermann et al., 2008; Knapp et al., 2018). Given the characteristics of different data, integrated multi-source and multi-scale data might provide a viable path to improve spatially explicit estimates of biomass over large areas (Blackard et al., 2008; Kindermann et al., 2008; Huang et al., 2019).

Although the advantages of combining satellite-based remote sensing and inventory datasets are obvious, it has apparent discrepancies in terms of the forest characteristics (such as forest area and volume) and the spatial resolutions of the source data (Kindermann et al., 2008; Huang et al., 2019). Therefore, the forest cover proportion map may be a good bridge to link forest inventory and remote sensing data using the methodology developed by Päivinen et al. (2009). The NOAA-based forest cover proportion map was calibrated and the distribution of forest biomass was estimated based on forest inventories in Europe (Päivinen et al., 2009). This methodology can estimate the actual forest cover objectively within a pixel and has been used in other recent studies (Hansen et al., 2013; De Jong et al., 2013; Du et al., 2014). Therefore, combining calibrated forest cover proportion maps with NDVI maximum values which represents the best state of forest growth would be the effective method to predict of forest C storage over the past few decades.

Mapping the spatial pattern of large-scale forest biomass by combining multi-source data can be used to verify the simulation results for process-based carbon cycle models (Le Toan et al., 2011). Here, we calibrated forest cover proportion maps and estimated the forest C storage and C density using the data of the statistical reports from eight national forest inventories. We next spatially downscaled the forest biomass map of China at 1 km resolution using multi-source data (the calibrated forest cover proportion map, NDVI data derived from the NOAA/AVHRR land dataset and statistically derived forest inventory biomass C stock estimates) from 1977 to 2018. Using this approach, we examined the spatiotemporal variation of forest biomass carbon sinks and biomass carbon density to figure out the possible factors that affect forest biomass and the effects of afforestation on forest biomass dynamics in China during the past four decades.

2. Data and methods

2.1. Data sources

2.1.1. Forest inventory data

In recent decades, China has periodically conducted national-level forest resource inventories. These inventories report information on forest area and timber volume by age group and forest type for all provinces. In this study, we used national forest inventory datasets for 8 periods (1977–1981, 1984–1988, 1989–1993, 1994–1998, 1999–2003, 2004–2008, 2009–2013 and 2014–2018), where China's forests are divided into forest stands (including natural and planted forests), economic forests, woodlands, and other forests (Chinese Ministry of Forestry, 1982, 1989, 1994, 1999, 2004, 2009, 2014, 2019). We used forest area and timber volume statistics of forest stands to calibrate the forest cover proportion data and estimate the forest biomass C density in 31 provinces. The forests in Hong Kong, Macao, and Taiwan were not included in this study due to the lack of data.

2.1.2. Forest cover proportion map

We used the forest cover proportion map that was extracted from the land-use maps and products that were based on Landsat 8 OLI and GF-2, and China's land-use remote sensing mapping system (Liu, 1996; Liu et al., 2003a, 2003b, 2010, 2014a, 2018). Using a high-resolution remote sensing-UAV-ground survey observation system, Liu et al. (2018) constructed the land-use vector status dataset via human-computer interaction, including land use in 1980, 1990, 1995, 2000, 2005, 2010 and 2015, based on priori geographic knowledge. Compared with traditional discrete classification data, this data set is more appropriate for describing forest cover changes (Liu et al., 2010, 2018).

The land use maps provided by Liu et al. (2018) distinguish the dominant land use types that include cultivated land, woodland, grassland, water area, residential land, and unused land at 30-m spatial resolution. In this study, we used these land use maps to generate a series of forest cover proportion maps with a spatial resolution of 1 km. To match the forest inventory periods, we used the average forest cover proportion in 1980 and 1990 to estimate forest coverage in 1985 because the land use maps did not cover this particular year.

2.1.3. NDVI data

The third generation Global Inventory Modeling and Mapping Studies Normalized Difference Vegetation Index (GIMMS NDVI3g) with a spatial resolution of 8×8 km and a 15-day temporal interval is used for establishing a correlation between biomass and annual maximum NDVI values at the provincial level (Tucker et al., 2004; Pinzon and Tucker, 2014). The GIMMS-NDVI3g dataset has been more carefully optimized than other NDVI datasets and is a very effective data source for large-scale studies of ecological processes (Myneni et al., 2001; Tucker et al., 2001; Piao et al., 2005; Militino et al., 2017). The disturbance from cloud and atmospheric effects and solar altitude angle can be further eliminated, and non-vegetation effects can be minimized using the maximum value composites (MVC) method (Holben, 1986).

2.1.4. Spatial distribution of forest projects in China

Since the late 1970s, China has carried out a series of national afforestation and reforestation projects, and meanwhile formulated a series of laws and regulations to promote forest restoration, conservation and afforestation. This led to an increase in forest coverage from 8.6% in the 1950s to 16.55% in 2000 (Fang et al., 2001; Li et al., 2016). Since 2000, China has intensified its efforts in afforestation and launched 8 forest protection projects.

We downloaded the map of forest projects from the Resource and Environment Data Cloud Platform (http://www.resdc.cn) created by the Institute of Geographic Sciences and Natural Resources Research (a part of the Chinese Academy of Sciences) (Fig. 1).

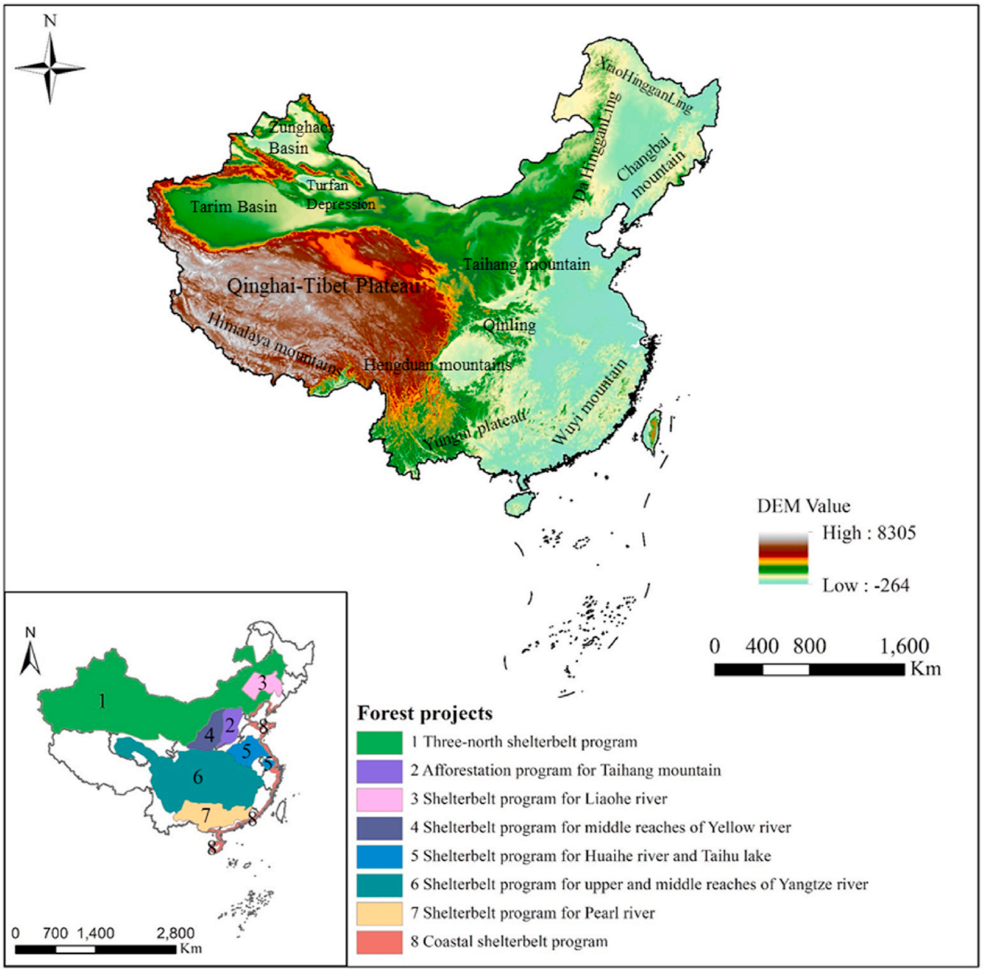

Fig. 1. Distribution map of the eight forest restoration programs.

2.2. Methods

In this study, we spatially downscaled the forest C stocks of China at a 1 km × 1 km spatial resolution using 8 national inventory datasets combined with the calibrated forest cover proportion maps and the GIMMS NDVI3g data during the period 1977–2018 (Appendix S1).

The whole process is divided into three phases: (1) the estimation of forest biomass C stocks from 1977 to 2018; (2) forest cover proportion calibration; and (3) the downscaling of forest biomass C density. The land use maps and GIMMS-NDVI3g datasets corresponding to the 8 forest inventories are shown in Appendix S2.

The 8-km GIMMS NDVI time series is first gap-filled and smoothed by the Savitzky-Golay filter (Chen et al., 2004; Yang et al., 2019), and the reconstructed data need to be resampled to the resolution of 1 km before downscaling. The annual maximum NDVI within one year is obtained and then all the annual maximum NDVI values in each inventory period are averaged to get the mean annual maximum (MAM) NDVI.

2.2.1. Biomass C estimation of forest stands

The biomass C stocks of forest stands were calculated using the refined Continuous Biomass Expansion Factor (CBEF) model with parameters for each forest type taken from Zhang et al. (2013) and Zhao et al. (2019). This method uses the allometric equation connecting biomass C stocks and timber volume prepared by Fang et al. (1998, 2001). Zhang et al. (2013) collected biomass measurements from 3543 forest plots and used these data with the published literature to improve the parameters of the model and Zhao et al. (2019) collected fractions of C (CF) from the published literature for each forest type, such that:

$$B = (a \cdot V + b) \cdot CF \tag{1}$$

where B is the total stand biomass C stocks (Mg ha^{-1}); V is the stand volume (m^3 ha^{-1}); CF is the C fraction of each forest type, and a and b are coefficients for specific forest types.

The canopy coverage threshold used to delineate forests stands was changed from >30% to >20% in China after 1994. In this study, we used the method developed by Fang et al. (2007) to correct the forest area and biomass C stocks that were calculated using the inventories before 1994 at the provincial level for studying the temporal dynamics of forest biomass C stocks.

2.2.2. Forest area calibration

We used the method of Päivinen et al. (2009) to reduce the discrepancies between the forest area estimates generated from forest inventory and land use remote sensing data regionally (Fig. 2a). This method retains the accuracy of the forest inventory data and the spatial distribution information provided by remote sensing. We classified land use types in a pixel into two categories (i.e., forest and non-forest), and obtained forest cover maps for each inventory period with pixel values ranging from 0 to 100% (Fig. 2b). That is, two raster layers representing the forest and non-forest cover types, respectively, were prepared for each inventory period for which the values in the pixels in the two raster layers add up to 100%. All the proportion maps were transformed to the Albers Equal-Area projection for further forest area calibration.

The main principle of the algorithm was to match the mean forest coverage estimated from the image within a region (e.g., province) to

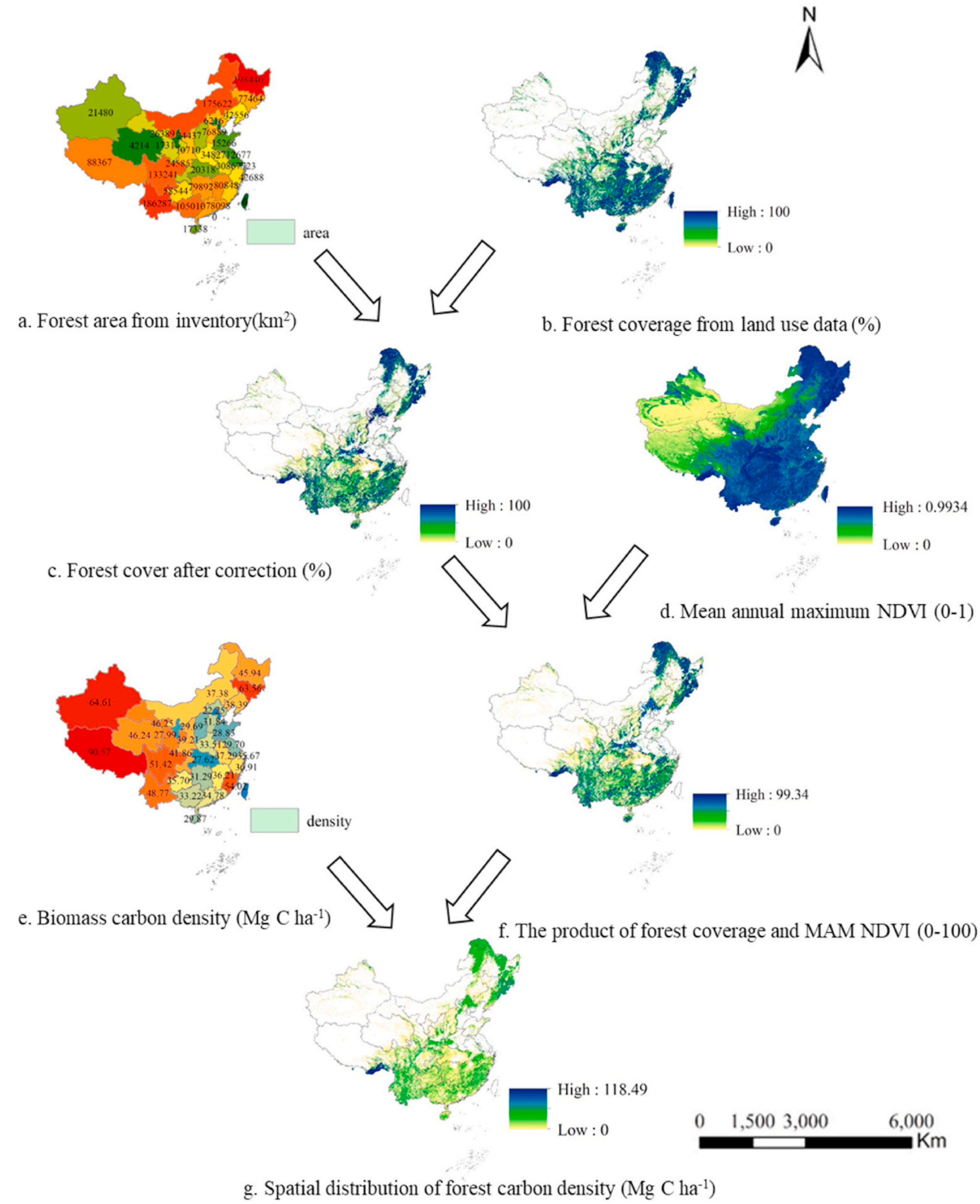

Fig. 2. Schematic diagram showing the maps used for downscaling forest biomass density (2014–2018, for example).

that from the inventory statistics to the extent possible by adjusting the forest and non-forest cover proportion in each pixel (Päivinen et al., 2009). Because the forest inventory takes the province as the unit of analysis, the procedure was conducted per province in all periods. The algorithm of the forest area calibration process was expressed by the following equation:

$$x_i^c = x_i \frac{X}{\overline{x}} \tag{2}$$

where i represents the pixel, x_i is the proportion value for the forest in a pixel (i) in a province (from 0 to 100%), X is the accurate average forest cover proportion in the same province based on forest inventory data, $\overline{x}$ represents the image-estimated mean coverage for forest in the province; and x_i^c is the adjusted proportion for forest in pixel (i).

To confirm the sum of calibrated forest and non-forest $(1 - x_i)$ is 100% for each pixel, the sum value is scaled by deriving a ratio (w_i) for each pixel:

$$W_i = \frac{1}{(1 - x_i)^c + x_i^c} \tag{3}$$

$$x_i^{wc} = W_i {}^* x_i^c \tag{4}$$

$$z = \frac{\left|\overline{x_i^{wc}} - X\right|}{X} \tag{5}$$

where x_i^{wc} is the adjusted proportion for the forest cover in a pixel (i) in one calculation; $\overline{x_i^{wc}}$ is the adjusted mean proportion for the forest in the province; and z represents the forest cover threshold value from the forest inventory statistics and that estimated from the calibrated image. In this study, the threshold value z was set to 0.01 for all provinces in all periods.

This algorithm is repeated until the value z is less than 0.01 in the province. For some provinces in which the forest cover proportion maps could not be calibrated or were not close to the value from the inventory statistics, we constrained the maximum calibration iterations to 100 to save time. Ultimately, we obtained the national calibrated forest cover proportion maps in sequence in all periods when the process was stopped for all provinces (Fig. 2c). The calibrated forest cover proportion maps are consistent with the inventory statistics for the past 40 years.

2.2.3. Downscaling

The downscaling of the forest C stocks based on the calibrated forest cover proportion maps was carried out next. Downscaling is used to transform large-scale, coarse resolution information into regional-scale, high-resolution information in many other related fields (e.g., Piao et al., 2005, 2009; Kindermann et al., 2008; Jia et al., 2011; Su et al., 2016). In general, forest inventory statistics can provide coarse resolution information, whereas remote sensing can reflect the spatially explicit information of forests at a high spatial resolution (Piao et al., 2005, 2009). Forest biomass C density was proportional to the forest coverage area or the MAM NDVI value at national, provincial and county scales (Piao et al., 2005; Du et al., 2014). In this study, we found a good relationship between forest biomass C stocks and the product of the total (the sum of *"forest coverage* MAM NDVI"*) forest coverage area and MAM NDVI among all provinces through the corresponding statistics in all provinces and all inventory periods (Fig. 3).

That is, the calibrated forest cover proportion maps and MAM NDVI can effectively reflect the spatial distribution of biomass C stocks, and therefore these combined datasets allow downscaling forest biomass C stocks from regional-based statistics to pixel-based estimates with a 1 km spatial resolution (Fig. 2g). In this study, the downscaling process was also conducted per province by the following equation:

$$B_i = \frac{B}{\sum_{i=1}^{i=n}[A_i * G_i]S} A_i * G_i \tag{6}$$

where B_i is the forest biomass C in pixel (i) (Mg C ha^{-1}); n is the number of pixels in a province from the calibrated map; B is the total forest biomass C of a province from the forestry inventory (Mg C); A_i is the forest area proportion of a province estimated from the calibrated map in a pixel (i)(0–1), which also matched the inventory statistics; G_i is the mean annual maximum NDVI value in a pixel (i) (−1–1); and s is the area of a pixel (100 ha).

3. Results

3.1. Forest biomass C sinks over the past 4 decades

The forest area increased from 11,660.47 × 10^4 ha during the period 1977–1981 to 17,988.85 × 10^4 ha during the period 2014–2018, growing by 1.47% per year on average (Table 1). Meanwhile, the forest biomass C stocks of forest stands increased with some fluctuations from 4128.50 to 7906.23 Tg C from 1977 to 1981 to 2014–2018, indicating an average rate of biomass C sequestration of 102.10 Tg C year^{-1}

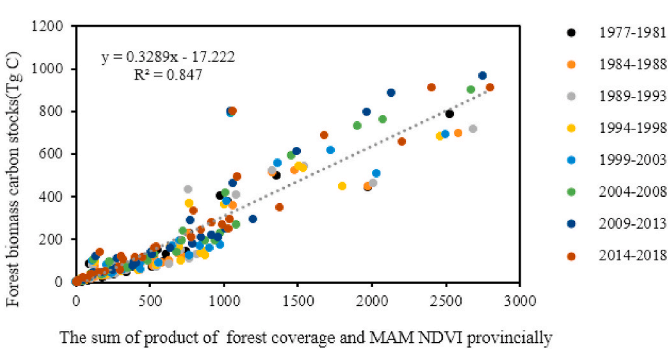

Fig. 3. Relationship between the sum of the product of the forest coverage and MAM NDVI and forest biomass C stocks at the provincial scale for all periods.

Table 1
Summary of forest variables in eight inventory periods.

	Area (10^{4}ha)	C stock (Tg C)	Density (Mg C ha^{-1})	Sink (Tg C yr^{-1})
1977–1981	11660.47	4128.50	35.41	–
1984–1988	12452.83	4161.49	33.42	4.71
1989–1993	13216.01	4510.46	34.13	69.79
1994–1998	12919.94	4478.91	34.67	−6.31
1999–2003	14278.67	5375.01	37.64	179.22
2004–2008	15558.99	6629.81	42.61	250.96
2009–2013	16460.35	7375.14	44.81	149.06
2014–2018	17988.85	7906.23	43.95	106.22
1977–2018	–	–	–	102.10

(Table 1). From 1977 to 2018, the C density of forest stands decreased slightly during the first four periods but later increased, leading to an average rate of change of 0.65% per year, and an overall change in density from 35.41 to 43.95 Mg C ha^{-1} from 1977 to 1981 to 2014–2018.

There are some substantial regional discrepancies in both the forest area and stocks of forest stands over time in China (see Appendices S3, S4, S5). The largest increases in forest area (415%) occurred in Hebei province from 1977 to 2018. The largest increases in forest biomass C density occurred in Shanghai province (266%) during the study period while Tibet has the largest biomass C density with 94.67 Mg C ha^{-1} during the period 2004–2008 (Appendix S4). The largest increases in forest biomass C stocks (975%) occurred in Hebei province from 1977 to 2018. Heilongjiang has the largest biomass C stocks with 966.18 Tg C during the period 2009–2013 (Appendix S5). In the recent period 2014–2018, Heilongjiang has the largest forest area with 198,440 km^2 and Fujian has the highest forest coverage of 51% (Appendix S3).

3.2. Calibration of forest area

To illustrate the impact of the calibration method, we compared the calibrated forest cover against the initial forest cover which had not been processed by the forest area calibration, as shown in Fig. 4. The forest areas from the forest inventory and forest cover map differed tremendously at the provincial level. After the calibration process, the regional discrepancies between the forest inventory statistics and raster representation were generally reduced. The calibration results were satisfactory and the absolute forest area estimates between them were nearly the same at both the provincial and national levels (Fig. 4). All of the provinces were calibrated successfully in the eight inventory periods except for the provinces with red numbers in Appendix S7, where the number of iterations reached 100.

We show the change of forest cover proportion before and after the forest area was calibrated, taking four provinces in different periods as an example (Fig. 5). In Guangxi province during period 1984–1988, the forest coverage rate using land use remote sensing data was 65.67%, while the coverage rate using the national forest inventory was 21.83%, and the final corrected rate was 22.05%. In Shaanxi province during the period 2014–2018, the forest coverage rate using land use remote sensing data was 23.2%, while the coverage rate using the national forest inventory was 34.4%, and the final corrected rate was 34.07% (Fig. 5, Appendix S3, S6, S7).

In addition to the above two cases of successful correction, there are also two cases with poor results. In Jiangsu province during the period 2014–2018, there were too few forest pixels to match the forest area estimated with the statistics, and all of the forest pixel values were adjusted to 100% (Fig. 5c1, c2). However, there is still a 17% gap between the forest inventory and the corrected forest cover map. The same situation applies to Hainan (15%, 2014–2018), Hebei (6%, 2014–2018), Shanghai (37%, 1989–1993) and Tianjin (6%, 1977–1981) provinces in one or more periods (Appendices S3, S7). The other scenario is there were more forest pixels than the forest area statistics for some periods in

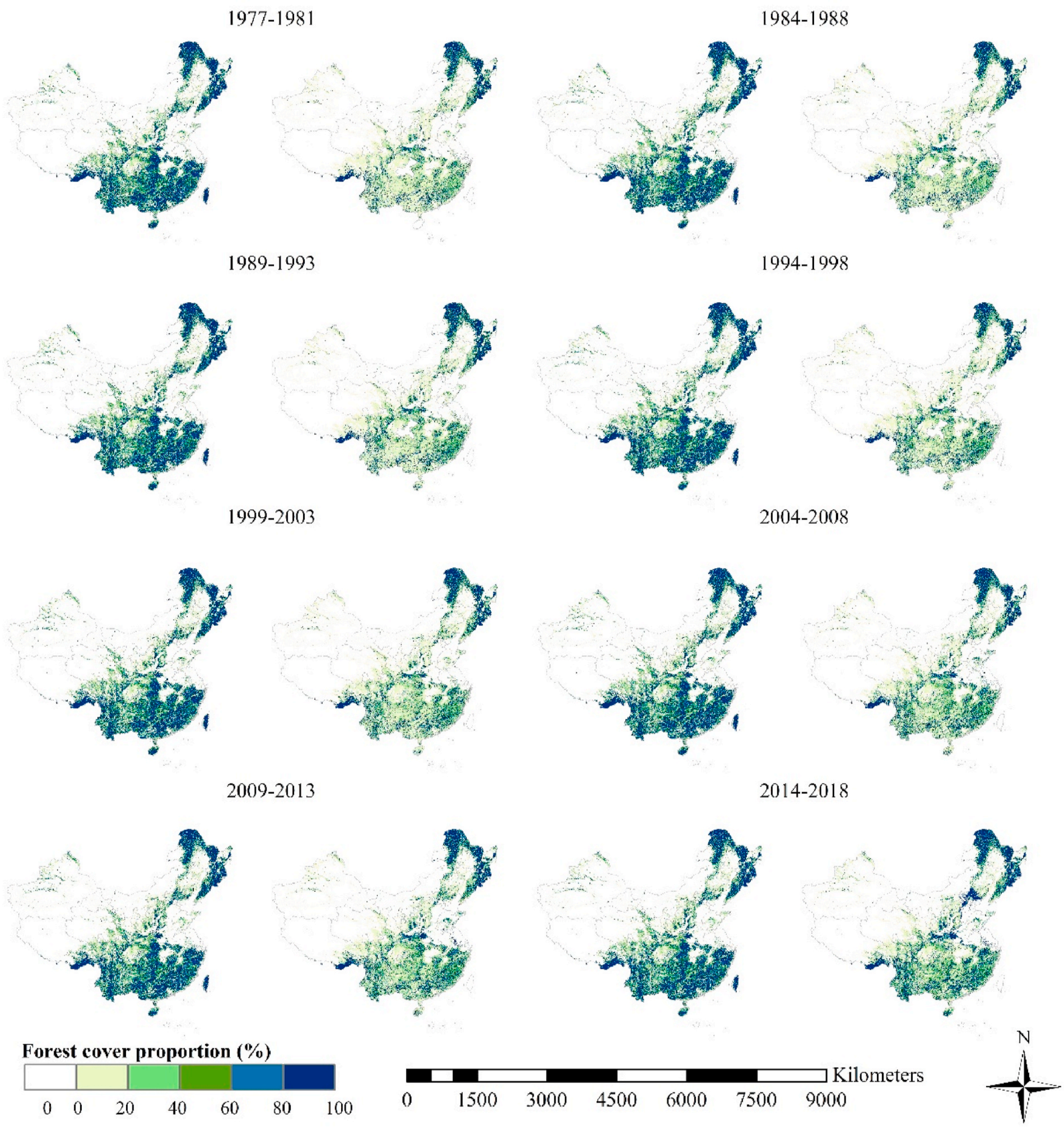

Fig. 4. Comparison of before and after calibrated forest cover proportion map. For each set of graphs, the left and right figures are initial and calibrated forest cover proportion maps, respectively. Hong Kong, Macao and Taiwan were not included in this study due to the lack of data.

Tibet province during the period 1994–1998 (Fig. 5d1, d2). The forest pixel values were adjusted to 0 to match the statistics in these instances but this still left a 22–55% difference in Tibet province between the forest inventory and corrected forest cover map estimates. The same situation occurred in Beijing during the period 1999–2003, and there was still a gap of 16% difference.

3.3. Spatial distribution of forest biomass C density

Combining the calibrated forest cover proportion map, NDVI data and inventory statistics, we estimated the distribution of forest biomass C at the pixel level for the eight periods (Fig. 6).

On the whole, forest biomass C was mainly distributed in the northeastern, southern and southwestern regions of China, and high biomass density occurred in the Da Hinggan, XiaoHingganLing, Changbai and Hengduan mountains (Fig. 6). The maximum forest biomass C densities in the aforementioned maps were 129.53, 82.53, 99.79, 102.67, 121.56, 118.17, 121.32, 118.49 Mg C ha^{-1} from 1977 to 2018 (Fig. 6).

From Fig. 6, we can observe that the forest C density gradually increased in southern Tibet owing to forest development. However, forest biomass C density has gradually decreased since the 1980s in the northeastern region, and especially in the XiaoHingganLing and Changbai mountain areas before rising again from 2000 onwards. The C density of forests has also increased in the Wuyishan, Taihang and Qinling mountains during this later period.

In the past 40 years, the forest biomass C density of China has gradually increased (Fig. 7). Due to the growth of forests, the frequency of the high forest biomass C density showed a significant increase after 2000; forest C densities >60 Mg C ha^{-1} increased from 1.9% in

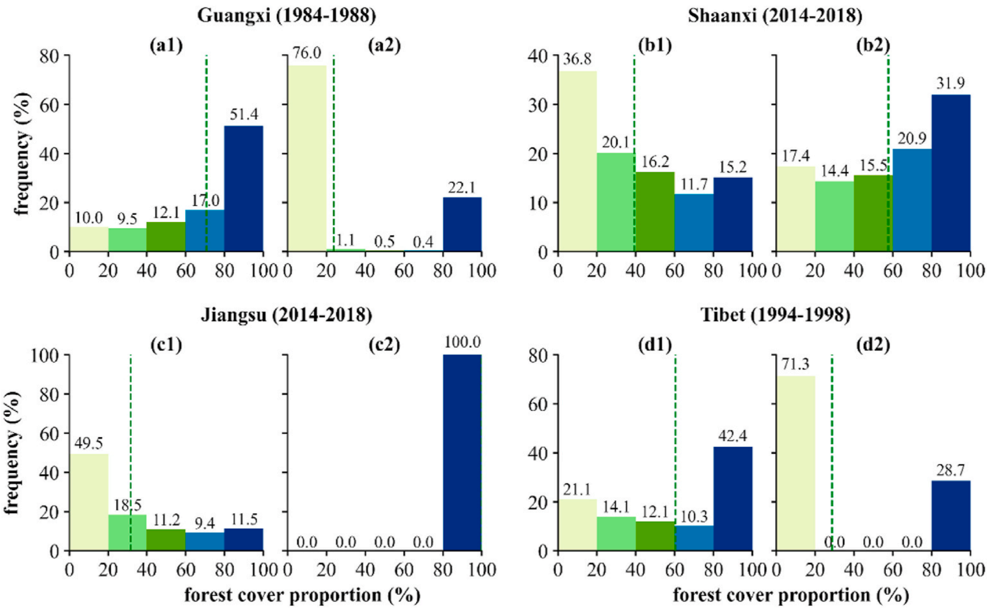

Fig. 5. Histogram of frequency distribution of forest cover proportion before (a1, b1, c1, d1) and after (a2, b2, c2, d2) calibration in Guangxi, Shaanxi, Jiangsu, and Tibet provinces.

1999–2003 to 3.3% in 2014–2018. Correspondingly, the low forest biomass C density decreased gradually and the frequency of forest biomass C densities < 20 Mg C ha^{-1} decreased from 72.3% in 1999–2003 to 55.1% in 2014–2018 (Fig. 7).

3.4. Spatial distribution of forest C sinks

In order to more intuitively see the change of forest biomass over time, we generated the distribution map of forest biomass C sinks in the three periods of 1977–1998, 1999–2018 and 1977–2018, based on the forest biomass C density distribution map (Fig. 8).

These maps show that forest biomass C stocks decreased by $\geq$ 5.54 Mg ha^{-1} yr^{-1} during 1977–1998 in the northeastern, most of the northern and a small part of the southern regions of China, which contain 29.4% of all forest. The forest biomass C stocks increased by 4.90 Mg ha^{-1} yr^{-1} in the south and part of the Qinghai-Tibet Plateau of China during the first four forest inventory periods (Fig. 8). In the forest-covered areas of China, 30.2% of the forest C sinks showed negative growth during 1977–1998, while in the areas with increasing forest C sinks, the majority of the areas (59.5%) showed slow growth, less than 0.25 Mg ha^{-1} yr^{-1} (Fig. 9).

Since 2000, forest biomass C stocks have increased in most of China with a maximum of 4.27 Mg ha^{-1} yr^{-1}, There are two exception: Hubei province where the forest biomass C stocks declined by two-thirds in this last period and the Tibetan Plateau with forest C density losses starting at −3.82 Mg ha^{-1} yr^{-1} (Appendix S5). In the forest-covered areas of China during the period 1999–2018, 41.3% of the forest C sinks grew more than 0.5 Mg ha^{-1} yr^{-1} (Fig. 9).

On the whole, forest biomass C stocks increased in the whole county from 1977 to 2018 with the exception of Hubei province (with losses of −2.32 Mg ha^{-1} yr^{-1} or more) and the highest rate of increase of forest C stocks occurring on the south Tibetan Plateau (with a maximum of 3.13 Mg ha^{-1} yr^{-1}). In the forest-covered areas of China, 93.8% of the forest has functioned as a C sink, and 50% of the forest C sinks have sequestered between 0 and 0.25 Mg ha^{-1} yr^{-1} during the past 40 years (Fig. 9).

4. Discussion

4.1. Calibration of forest area under different situations

The forest area calibration method overcomes the systematic underestimation of sparse forests and overestimation of dense forests. The benefits of this iterative method are that it minimizes the deviations between the remote sensing- and ground-based values, and guarantees the calibrated forest cover proportions in all pixels fall within the range of 0–100%, and that the sums of forest and non-forest cover proportions always equal 100%. To display the process of forest cover proportion calibration more intuitively, we constructed two comparison charts (Fig. 10a and b).

Radians represent the discrepancies between the land use remote sensing data and calibrated forest cover proportions. The smaller the radians, the smaller the discrepancies and at the same time, the fewer the iterations.

4.2. Spatiotemporal changes in forest biomass C stocks

Forest biomass C stocks increased from 4128.50 in 1977–1981 to 7906.23 Tg C in 2014–2018, indicating China's forests functioned as C sinks in the past 4 decades (Table 1, Appendix S5). The increase in forest C stocks could be attributed to the expansion of forest areas due to the implementation of afforestation and ecological restoration programs in China (Fang et al., 2001, 2007; FAO, 2005). Planted forests contributed a great deal to forest C stocks (Fang et al., 2014; Li et al., 2016). However, in these studies the distribution of forest biomass C stocks was only estimated at the provincial level, and the exact distribution was not known (Fang et al., 2001, 2007; Guo et al., 2010; Zhang et al., 2013, 2015). For example, the forest C stocks in Tibet in this study are mainly distributed in a small southern part of the Qinghai-Tibet Plateau (Sun et al., 2016). The spatiotemporal patterns of forest C stocks can be more clearly detected using the forest distribution ratio maps combined with NDVI data and forest inventory data to obtain the distribution of forest C stocks at the pixel level.

The highest biomass C stocks of China's forest are mainly distributed in the DaHingganLing, XiaoHingganLing, and Changbai mountains in the northeast, the Taihang and Qinling mountains in the north, the Hengduan mountains (Yungui plateau) in the southwest, and the Wuyi

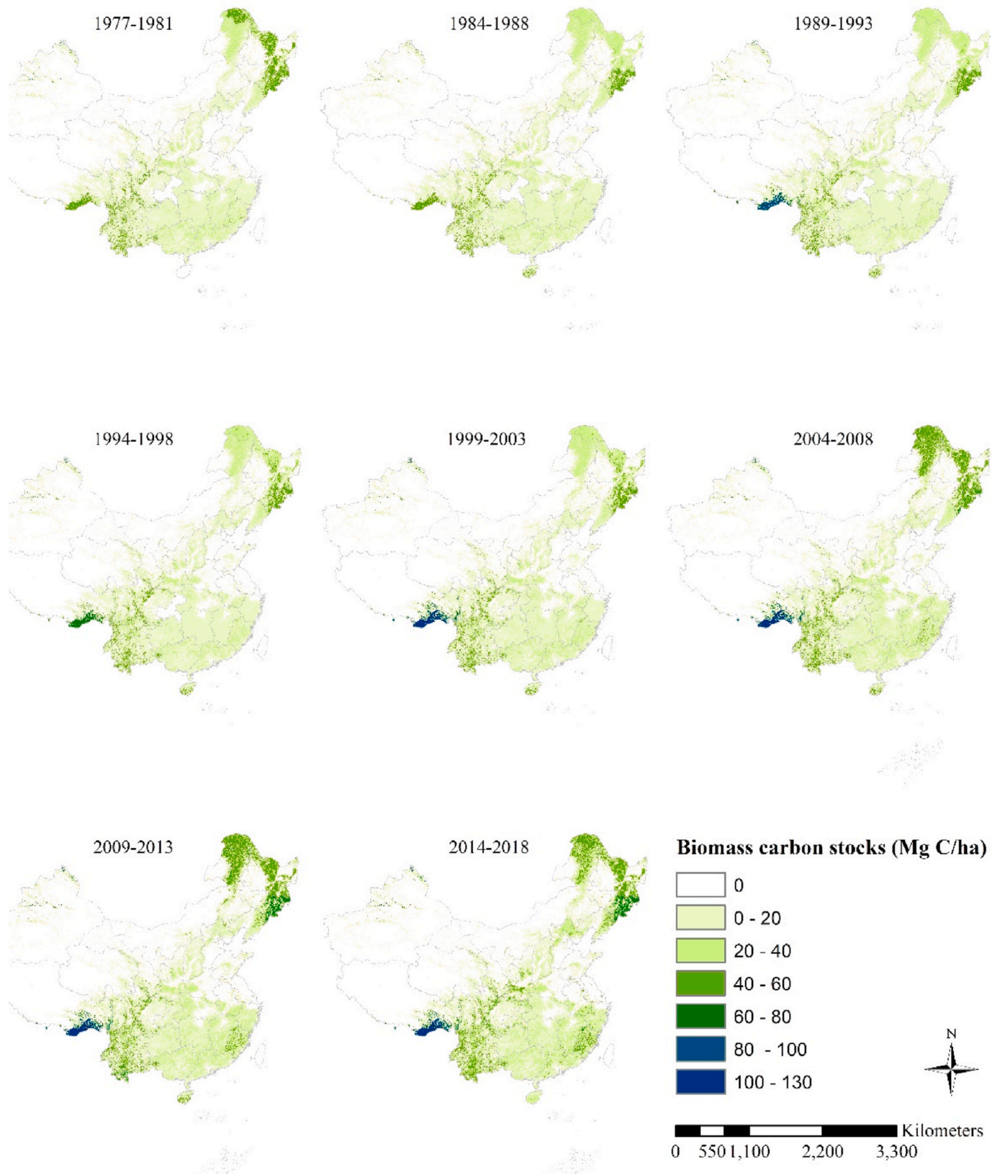

Fig. 6. Changes in biomass C stocks of China's forest from 1977 to 2018.

mountains in the south (Fig. 6). China has carried out a series of ecological protection programs since 1998, thus taking 1998 as a pivot, the changes of forest biomass C storage in China can be divided into two stages (Li et al., 2016). In the 1980s, due to the harvest of mature forests and deforestation in the northeast and rapid urbanization in the southeast, forest C stocks in these two areas significantly declined. But on the Tibet Plateau, which was less affected by human disturbance, forest C stocks increased due to forest development (Fang et al., 2001; Du et al., 2014; He et al., 2017). During the second stage, China implemented a series of forest restoration and protection projects, including six major forestry projects: (1) the Three-North Protection Forest System (2000); (2) the Natural Forest Conservation Projects (2000); (3) the Wildlife and Nature Reserve Construction Projects (2001); (4) the Fast-growing Forests in Key Areas Projects (2002); (5) the Grain for Green Project (2002); and (6) the Beijing–Tianjin–Hebei Sandstorm Source Treatment Project (Lei, 2005; Wang et al., 2007; Li et al., 2016). Forest biomass C began to increase due to rapid and concentrated afforestation projects, especially in the northeast, followed by the northern and southern regions. However, forest C density gradually reached saturation in the south of the Qinghai-Tibet Plateau owing to forest growth and the forest biomass C has not changed much in the past few years (Keith et al., 2009; Liu et al., 2014b; He et al., 2017).

In general, forest biomass C in the southern and northern regions is lower than in the northeastern and southwestern regions. The main reason is that there are more planted forests in the southern and northern regions than in the northeastern and southwestern regions, and most of the trees are still at young and middle-ages with low C density (Li et al., 2016; Qiu et al., 2020).

4.3. The effects of forest project to C sinks

Forest protection projects have been implemented since 1998, and China is credited with having made a significant contribution to regional and global C sinks in recent decades (Li et al., 2016; Wang et al., 2018; Huang et al., 2019; Chen et al., 2019). Therefore, in order to correctly assess the effects of relevant forestry policies and programs on forest biomass C sequestration, we analyzed the change of forest C storage in the areas covered by the eight major forest programs during all eight forest inventory periods.

Forests programs covered 68.64% of the country, and accounted for

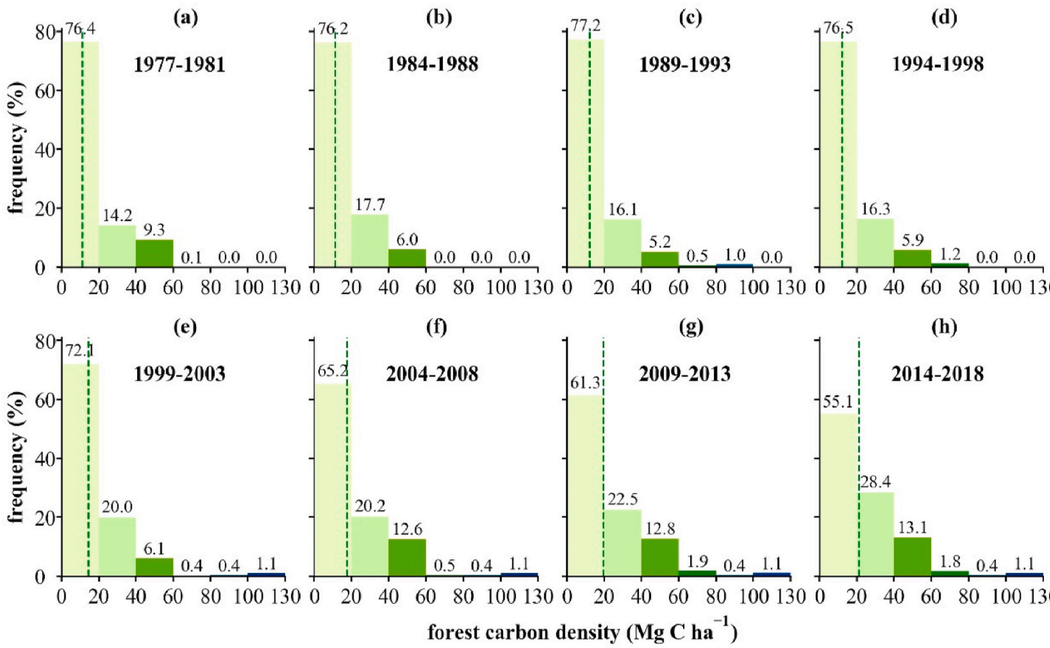

Fig. 7. The frequency distribution histogram of biomass C density of China's forest from 1977 to 2018.

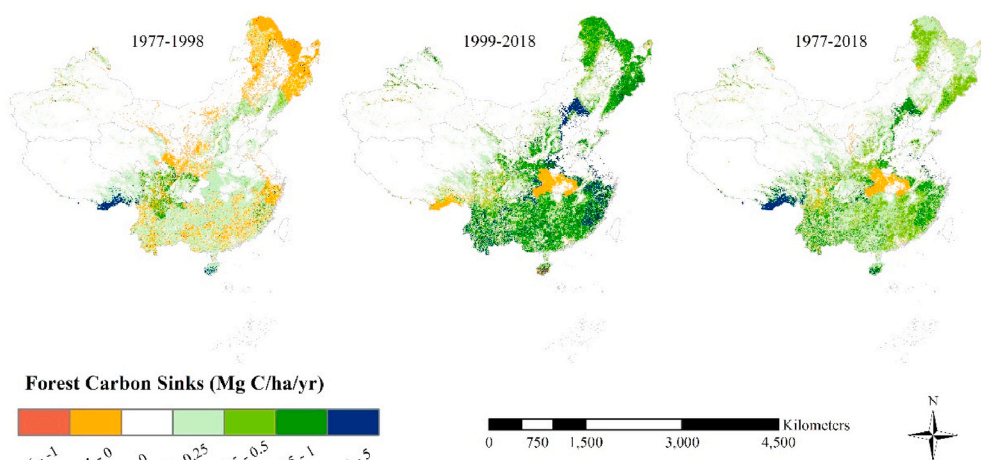

Fig. 8. Spatial distribution of forest C sinks in China for three periods.

44.08%–50.93% of C stocks in China from 1977 to 2018. From Fig. 11, we can see that the forest C sequestration rate was tiny in the areas where the eight major forest programs were implemented during the first four periods. Since 1998, the forest C stocks of the forest program areas began to increase linearly, especially in the Shelterbelt program implementation in the upper and middle reaches of the Yangtze River. This particular project added 952.19 Tg C and the Shelterbelt program for the Huaihe River and Taihu Lake increased the C stocks four-fold (417%) in these areas from 1998 to 2018 (Fig. 11). The overall rate of increase of forest C storage in the eight major forests programs area (95%) is higher than that for the country as a whole (77%) since 1998 (Fig. 11, Appendix S2). All ecological projects lead to the increased forest area and forest biomass carbon density, which caused forest biomass carbon changes. Specifically, the largest increase in forest area happens in the "Shelterbelt program for upper and middle reaches of Yangtze river" project, with an increased area of $2078*10^4$ ha. In the "Shelterbelt program for Huaihe river and Taihu lake" project, the forest area and forest biomass carbon density increased by 165% and 116%, respectively (Appendix S11, S12).

The implementation of these forest projects can also improve the environments in fragile ecological areas and the provision of ecosystem services. These projects could reduce soil erosion and water losses, increase soil fertility, strengthen forest C sequestration, help the forest to accumulate nutrients and purify the atmosphere (Wang et al., 2018; Huang et al., 2019). China's forest coverage will be 24% in 2030 because of the medium- and long-term state forestry development plans (Xu et al., 2010), and the potential for further forest biomass C sequestration in the future is high as well (Fang et al., 2018; Lu et al., 2018; Zhao et al., 2019).

4.4. Uncertainty

The method for downscaling forest C density using forest biomass C stocks and forest coverage proportion multiplied by NDVI was validated using 8 forest inventory datasets for 31 provinces. Overall, the forest C density and spatial pattern of forest C stocks in this study were consistent with previous studies (Zhang et al., 2013, 2015; Du et al., 2014; Su et al., 2016; Huang et al., 2019). However, there were some estimates

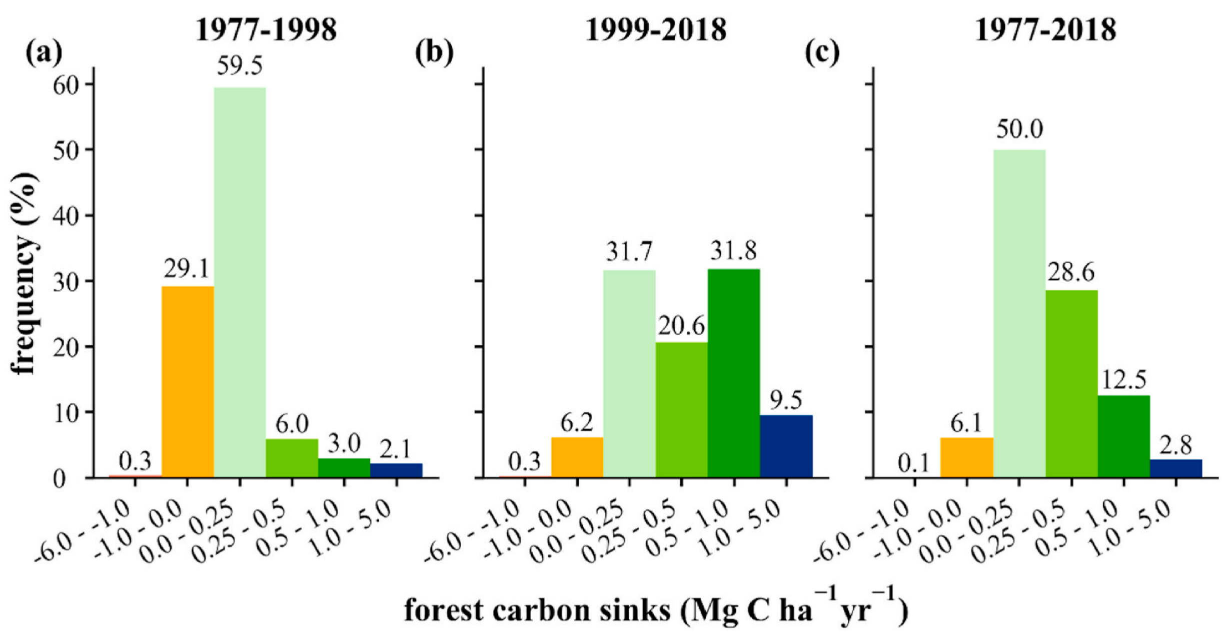

Fig. 9. The frequency distribution histogram of forest C sinks in China for three periods.

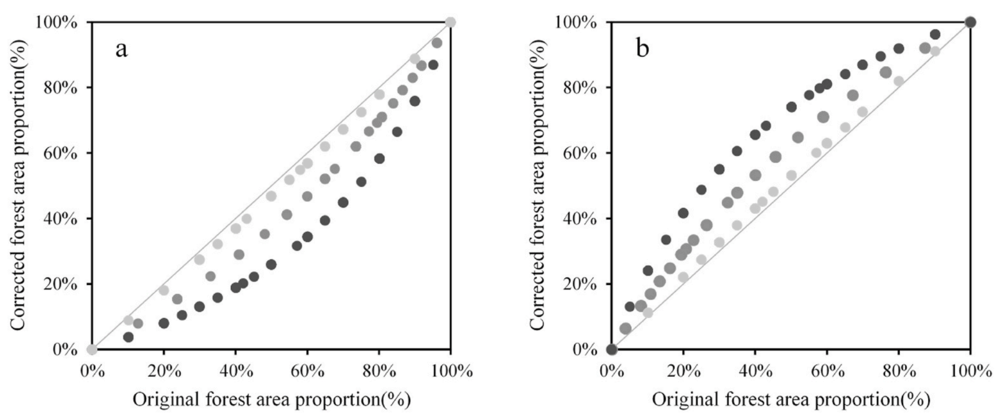

Fig. 10. Calibration of forest coverage grid values in two different scenarios: a and b represent the cases where the initial forest cover proportion is too large or too small, and the x and y axes represent the initial and calibrated forest cover proportions. The gradient of color represents the difference between the initial and calibrated forest cover proportions, the darker the color, the larger the difference. The grey line represents the 1:1 line.

uncertainties due to the complexity of forest types, stand age, density, and other ecosystem variability.

Specifically, although it is recognized that forest inventory data is one of the most reliable data sources for calculating forest C stocks (Smith et al., 2002), there were some uncertainties resulting from the changes in the definitions of forests (the canopy cover threshold from 0.3 to 0.2) (Fang et al., 2007), the variations in inventory methods, and the paucity of sample data (Pan et al., 2004). Besides, the empirical relationships embedded in the CBEF methods also gloss over some of the variability, which may affect the biomass estimates (Zhang et al., 2013; Zhao et al., 2019). Moreover, the forest cover proportion maps from land-use datasets are based on visual interpretation of satellite imagery, which may not be completely consistent with the national forest inventories (Liu et al., 2010, 2018). In addition, the resampling of GIMMS NDVI data from 8 km to 1 km, may also introduce more or less estimation uncertainties. The *R* value between forest biomass C stocks and the product of forest coverage and MAM NDVI provincially is 0.92, meanwhile, the non-linear relationship between NDVI and leaf area index (LAI) at high LAI values leads to imprecise estimation of forest C stocks (Chang et al., 2019). Therefore, using forest area and biomass C stocks from the statistics of the national forest inventories within each province individually as constraints to calibrate the satellite-based forest cover map and downscale the forest biomass C distribution map may gloss over potential system deviation. Meanwhile, the forest C stocks might indicate abrupt changes along provincial boundaries where continuous forests may exist.

During the forest area calibration process, there are still some provinces that could not be corrected despite choosing a threshold value z set to 0.01. In Hainan province, for example, the area of forest in the satellite-based map was too small to match the statistics of forest national inventories. Owing to the spatial heterogeneity of the geographic regions, the system deviations among different provinces are somewhat different and the scaling transformations of forest area from some provinces (i.e., those with sparsely distributed forest) were not completely applicable to the others (i.e., those with widely distributed forest).

Notwithstanding these uncertainties, the result n of forest C stocks distribution in this study shows relatively high precision. This study provides a basis for comprehensive investigations of the forest C budget and the forest area's contributions to forest C sinks. These attributes mean that the results of this work can be used to help develop sustainable forest management policies in the face of climate change across

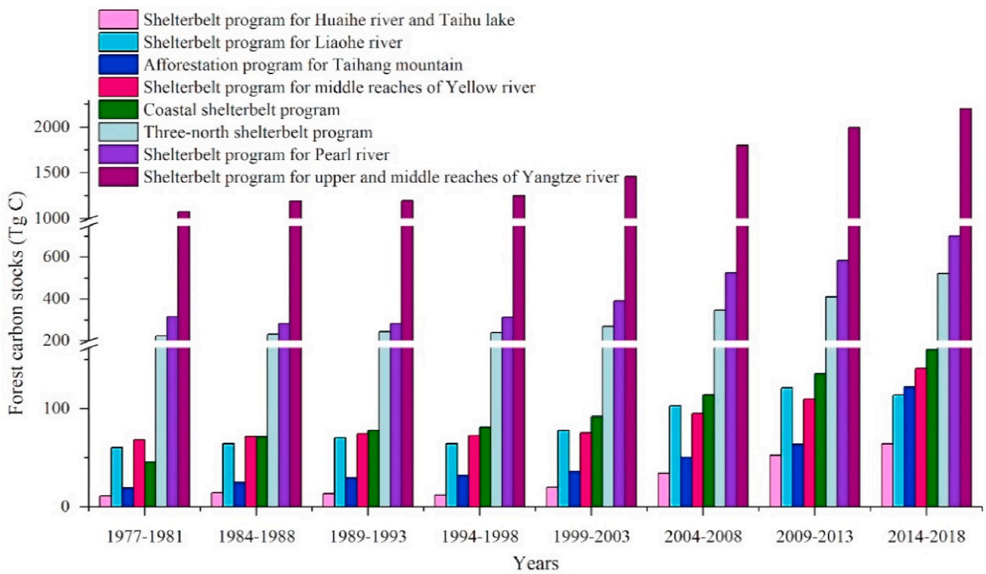

Fig. 11. Forest C sequestration of forest project regions from 1977 to 2018.

China.

5. Conclusions

In this research, we used a method to downscaling the forest biomass C density and sinks that matched the forest inventory data, based on multi-source dataset (e.g. forest inventory datasets, NDVI data, and land-use remote sensing mapping system data). The area and biomass C stocks of China's forest increased from 11,660.47*10^4 ha and 4128.50 Tg C to 17,988.85*10^4 ha and 7906.23 Tg C with C sinks of 102.10 Tg C yr^{-1} in 2018, respectively. The study improved spatiotemporal specificity and the ability to document the locations and magnitudes of the C sinks, which were mainly distributed in the northeast, southwest and southeast of China. Meanwhile, the study describe the spatiotemporal dynamics of C sinks, with increased C sequestration rates after 2000.

CRediT authorship contribution statement

Miaomiao Zhao: designed the research, Data curation, Writing – original draft. **Jilin Yang:** designed the research, Data curation, Writing – original draft, contributed to the implementation of forest area calibration. **Na Zhao:** contributed to the implementation of forest area calibration. **Luo Liu:** contributed to the implementation of forest area calibration. **Ling DU:** contributed to the implementation of forest area calibration. **Xiangming Xiao:** Formal analysis, provided valuable comments and suggestions on earlier drafts of the manuscripts. **Tianxiang Yue:** Formal analysis, provided valuable comments and suggestions on earlier drafts of the manuscripts. **John P. Wilson:** Formal analysis, provided valuable comments and suggestions on earlier drafts of the manuscripts.

Declaration of competing interest

The authors declare that they have no known competing financial interests or personal relationships that could have appeared to influence the work reported in this paper.

Acknowledgements

This work was supported by the Strategic Priority Research Program (A) of the Chinese Academy of Sciences (XDA20030203), National Natural Science Foundation of China (41930647), the Innovation Project of LREIS (O88RA600YA), China Scholarship Council (No.201804910728), and the Biodiversity Investigation, Observation and Assessment Program (2019–2023) of the Ministry of Ecology and Environment of China. We also thank the Resource and Environment Data Cloud Platform for providing the land use datasets and the map of forest projects (http://www.resdc.cn/).

Appendix A. Supplementary data

Supplementary data to this article can be found online at https://doi.org/10.1016/j.jclepro.2021.128274.

References

Arneth, A., Harrison, S.P., Zaehle, S., Tsigaridis, K., Menon, S., Bartlein, P.J., Feichter, J., Korhola, A., Kulmala, M., O'Donnell, D., Schurgers, G., Sorvari, S., Vesala, T., 2010. Terrestrial biogeochemical feedbacks in the climate system. Nat. Geosci. 3 (8), 525–532.

Babcock, C., Finley, A.O., Cook, B.D., Weiskittel, A., Woodall, C.W., 2016. Modeling forest biomass and growth: coupling long-term inventory and LiDAR data. Remote Sens. Environ. 182, 1–12.

Blackard, J.A., Finco, M.V., Helmer, E.H., et al., 2008. Mapping US forest biomass using nationwide forest inventory data and moderate resolution information. Remote Sens. Environ. 112, 1658–1677.

Bonan, G.B., 2008. Forests and climate change: forcings, feedbacks, and the climate benefits of forests. Science 320, 1444–1449.

Brown, S., 2002. Measuring carbon in forests: current status and future challenges. Environ. Pollut. 116, 363–372.

Chang, Q., Xiao, X., Jiao, W., Wu, X., Doughty, R., Wang, J., Du, L., Zou, Z., Qin, Y., 2019. Assessing consistency of spring phenology of snow-covered forests as estimated by vegetation indices, gross primary production, and solar-induced chlorophyll fluorescence. Agric. For. Meteorol. 275, 305–316.

Chen, H.Y.H., Luo, Y., 2015. Net aboveground biomass declines of four major forest types with forest ageing and climate change in western Canada's boreal forests. Global Change Biol. 21, 3675–3684.

Chen, J., Jönsson, P., Tamura, M., Gu, Z., Matsushita, B., Eklundh, L., 2004. A simple method for reconstructing a high-quality NDVI time-series data set based on the Savitzky–Golay filter. Rem. Sens. Environ. 91, 332–344.

Chen, C., Park, T., Wang, X., Piao, S., Xu, B., Chaturvedi, R.K., Fuchs, R., Brovkin, V., Ciais, P., Fensholt, R., Tømmervik, H., Bala, G., Zhu, Z., Nemani, R.R., Myneni, R.B., 2019. China and India lead in greening of the world through land-use management. Nat. Sustain. 2 (2), 122–129.

Chinese Ministry of Forestry, 1983, 1989, 1994, 2000, 2005, 2010, 2014, 2019. Forest Resource Statistics of China (1977–1981, 1984–1988, 1989–1993, 1994–1998, 1999–2003, 2004–2008, 2009-2013, 2014-2018. Department of Forest Resource and Management, Chinese Ministry of Forestry, Beijing, China.

De Jong, R., Schaepman, M.E., Furrer, R., de Bruin, S., Verburg, P.H., 2013. Spatial relationship between climatologies and changes in global vegetation activity. Global Change Biol. 19, 1953–1964.

Dixon, R.K., Brown, S., Houghton, R.A., et al., 1994. Carbon pools and flux of global forest ecosystems. Science 263, 185–190.

Du, L., Zhou, T., Zou, Z., et al., 2014. Mapping forest biomass using remote sensing and National Forest Inventory in China. Forests 5, 1267–1283.
Fang, J., Wang, G.G., Liu, G., Xu, S., 1998. Forest biomass of China: an estimate based on the biomass-volume relationship. Ecol. Appl. 8, 1084–1091.
Fang, J., Chen, A., Peng, C., Zhao, S., Ci, L., 2001. Changes in forest biomass carbon storage in China between 1949 and 1998. Science 292, 2320–2322.
Fang, J., Guo, Z., Piao, S., Chen, A., 2007. Terrestrial vegetation carbon sinks in China, 1981–2000. Sci. Chin. Ser. Earth Sci. 50, 1341–1350.
Fang, J., Guo, Z., Hu, H., Kato, T., Muraoka, H., Son, Y., 2014. Forest biomass carbon sinks in East Asia, with special reference to the relative contributions of forest expansion and forest growth. Global Change Biol. 20, 2019–2030.
Fang, J., Yu, G., Liu, L., Hu, S., Chapin, F.S., 2018. Climate change, human impacts, and carbon sequestration in China. Proc. Nat. Acad. Sci. USA 115 (16), 4015–4020.
FAO, Global Forest Resources Assessment, 2005. Progress towards Sustainable Forest Management. Food and Agriculture Organization, Rome, Italy.
Gong, P., 2012. Remote sensing of environmental change over China: a review. Chin. Sci. Bull. 57, 2793–2801.
Guo, Z., Fang, J., Pan, Y., Birdsey, R., 2010. Inventory-based estimates of forest biomass carbon stocks in China: a comparison of three methods. For. Ecol. Manag. 259, 1225–1231.
Hansen, M.C., Potapov, P.V., Moore, R., et al., 2013. High-resolution global maps of 21st-Century forest cover change. Science 342, 850–853.
He, N., Wen, D., Zhu, J., Tang, X., Xu, L., Zhang, L., Hu, H., Huang, M., Yu, G., 2017. Vegetation carbon sequestration in Chinese forests from 2010 to 2050. Global Change Biol. 23 (4), 1575–1584.
Holben, B.N., 1986. Characteristics of maximum value composite images from temporal AVHRR data. Int. J. Rem. Sens. 7, 1417–1434.
Huang, H., Liu, C., Wang, X., Zhou, X., Gong, P., 2019. Integration of multi-resource remotely sensed data and allometric models for forest aboveground biomass estimation in China. Remote Sens. Environ. 221, 225–234.
Jia, S., Zhu, W., Lu, A., Yan, T., 2011. A statistical spatial downscaling algorithm of TRMM precipitation based on NDVI and DEM in the Qaidam Basin of China. Remote Sens. Environ. 115, 3069–3079.
Ju, W.M., Chen, J.M., Harvey, D., Wang, S.Q., 2007. Future carbon balance of China's forests under climate change and increasing CO2. J. Environ. Manag. 85, 538–562.
Keith, H., Mackey, B., Lindenmayer, D.B., 2009. Re-evaluation of forest biomass carbon stocks and lessons from the world's most carbon-dense forests. Proc. Natl. Acad. Sci. U.S.A. 106, 11635–11640.
Kindermann, G.E., McCallum, I., Fritz, S., Obersteiner, M., 2008. A global forest growing stock, biomass and carbon map based on FAO statistics. Silva Fenn. 42, 387–396.
Knapp, N.R., Fischer Huth, A., 2018. Linking LiDAR and forest modeling to assess biomass estimation across scales and disturbance states. Remote Sens. Environ. 205, 199–209.
Le Toan, T., Quegan, S., Davidson, M.W.J., et al., 2011. The BIOMASS mission: mapping global forest biomass to better understand the terrestrial carbon cycle. Remote Sens. Environ. 115, 2850–2860.
Lei, J., 2005. Forest Resource of China. China Forestry Publishing House, Beijing.
Li, P., Zhu, J., Hu, H., Guo, Z., Pan, Y., Birdsey, R., Fang, J., 2016. The relative contributions of forest growth and areal expansion to forest biomass carbon. Biogeosciences 12 (12), 9587–9612.
Liu, J.Y., 1996. Macro-scale Survey and Dynamic Study of Natural Resources and Environment of China by Remote Sensing Beijing. China Science and Technology Press (in Chinese).
Liu, J.Y., Liu, M.L., Zhuang, D.F., et al., 2003a. Study on spatial pattern of land-use change in China during 1995–2000. Sci. China, Ser. A D 46, 373–384.
Liu, J.Y., Zhang, Z.X., Zhuang, D.F., et al., 2003b. A study on the spatial-temporal dynamic changes of land-use and driving forces analyses of China in the 1990s. Geogr. Res. 22, 1–12 (in Chinese).
Liu, J.Y., Zhang, Z.X., Xu, X.L., et al., 2010. Spatial patterns and driving forces of land use change in China during the early 21st century. J. Geogr. Sci. 20, 483–494.
Liu, J.Y., Kuang, W.H., Zhang, Z.X., et al., 2014a. Spatiotemporal characteristics, patterns, and causes of land-use changes in China since the late 1980s. J. Geogr. Sci. 24, 195–210.
Liu, Y., Yu, G., Wang, Q., Zhang, Y., Xu, Z., 2014b. Carbon carry capacity and carbon sequestration potential in China based on an integrated analysis of mature forest biomass. Sci. China Life Sci. 57, 1218–1229.
Liu, J.Y., Ning, J., Kuang, W.H., et al., 2018. Spatio-temporal patterns and characteristics of land-use change in China during 2010-2015. J. Geogr. Sci. 73, 789–802.
Lu, F., Hu, H., Sun, W., Zhu, J., Liu, G., Zhou, W., Zhang, Q., Shi, P., Liu, X., Wu, X., Zhang, L., Wei, X., Dai, L., Zhang, K., Sun, Y., Xue, S., Zhang, W., Xiong, D., Deng, L., Liu, B., Zhou, L., Zhang, C., Zheng, X., Cao, J., Huang, Y., He, N., Zhou, G., Bai, Y., Xie, Z., Tang, Z., Wu, B., Fang, J., Yu, G. Liu G., 2018. Effects of national ecological restoration projects on carbon sequestration in China from 2001 to 2010. Proc. Natl. Acad. Sci. U.S.A. 115 (16), 4039–4044.
Matasci, G.T., Hermosilla, M.A., Wulder, J.C., et al., 2018. Three decades of forest structural dynamics over Canada's forested ecosystems using Landsat time-series and lidar plots. Remote Sens. Environ. 216, 697–714.
Militino, A., Ugarte, M., Pérez-Goya, U., 2017. Stochastic spatio-temporal models for analysing NDVI distribution of GIMMS NDVI3g images. Rem. Sens. 9, 76.
Myneni, R.B.J., Dong, C.J., Tucker, R.K., et al., 2001. A large carbon sink in the woody biomass of Northern forests. Proc. Natl. Acad. Sci. U.S.A. 98, 14784–14789.
Päivinen, R., van Brusselen, J., Schuck, A., 2009. The growing stock of European forests using remote sensing and forest inventory data. Forestry 82, 479–490.
Pan, Y.D., Luo, T.X., Birdsey, R., Hom, J., Melillo, J., 2004. New estimates of carbon storage and sequestration in China's forests: effects of age-class and method on inventory-based carbon estimation. Clim. Chang. 67 (2–3), 211–236.
Pan, Y., Birdsey, R.A., Fang, J., Houghton, R., Kauppi, P.E., Kurz, W.A., Phillips, O.L., Shvidenko, A., Lewis, S.L., Canadell, J.G., Ciais, P., Jackson, R.B., Pacala, S.W., McGuire, A.D., Piao, S., Rautiainen, A., Sitch, S., Hayes, D., 2011. A large and persistent carbon sink in the world's forests. Science 333, 988–993.
Piao, S., Fang, J., Zhu, B., Tan, K., 2005. Forest biomass carbon stocks in China over the past 2 decades: estimation based on integrated inventory and satellite data. J. Geophys. Res. Biogeosci. 110 (G1).
Piao, S., Fang, J., Ciais, P., Peylin, P., Huang, Y., Sitch, S., Wang, T., 2009. The carbon balance of terrestrial ecosystems in China. Nature 458 (7241), 1009–1082.
Pinzon, J., Tucker, C., 2014. A non-stationary 1981–2012 AVHRR NDVI3g time series. Rem. Sens. 6, 6929–6960.
Qin, Y., Xiao, X., Dong, J., Zhang, Y., Wu, X., Shimabukuro, Y., Arai, E., Biradar, C., Wang, J., Zou, Z., Liu, F., Shi, Z., Doughty, R., Moore, B., 2019. Improved estimates of forest cover and loss in the Brazilian Amazon in 2000–2017. Nat. Sustain. 2, 764–772.
Qiu, Z., Feng, Z., Song, Y., Li, M., Zhang, P., 2020. Carbon sequestration potential of forest vegetation in China from 2003 to 2050: predicting forest vegetation growth based on climate and the environment. J. Clean. Prod. 252, 119715.
Rauste, Y., 2005. Multi-temporal JERS SAR data in boreal forest biomass mapping. Remote Sens. Environ. 97, 263–275.
Smith, J.E., Heath, L.S., Jenkins, J.C., 2002. Forest Tree Volume to Biomass Models and Estimates for Live and Standing Dead Trees of U.S. Forest. USDA Forest Service. Gen Tech Rep NE-298, Washington DC, p. p57.
Su, Y., Guo, Q., Xue, B., Hu, T., Alvarez, O., Tao, S., Fang, J., 2016. Spatial distribution of forest aboveground biomass in China: estimation through combination of spaceborne LiDAR, optical imagery, and forest inventory data. Remote Sens. Environ. 173, 187–199.
Sun, X., Wang, G., Huang, M., Chang, R., Ran, F., 2016. Forest biomass carbon stocks and variation in Tibet's carbon-dense forests from 2001 to 2050. Sci. Rep. 6.
Tucker, C.J., Slayback, D.A., Pinzon, J.E., Los, S.O., Myneni, R.B., Taylor, M.G., 2001. Higher northern latitude normalized difference vegetation index and growing season trends from 1982 to 1999. Int. J. Biometeorol. 45, 184–190.
Tucker, M.P., Nagle, N.J., Jennings, E.W., Ibsen, K.N., Aden, A., Nguyen, Q.A., Kim, K.H., Noll, S.L., 2004. Conversion of distiller's grain into fuel alcohol and a higher-value animal feed by dilute-acid pretreatment. Appl. Biochem. Biotechnol. 113–116, 1139–1159.
Wang, S., Chen, J.M., Ju, W.M., Feng, X., Chen, M., Chen, P., Yu, G., 2007. Carbon sinks and sources in China's forests during 1901-2001. J. Environ. Manag. 85 (3), 524–537.
Wang, K.B., Hu, D.F., Deng, J., Shangguan, Z.P., Deng, L., 2018. Biomass carbon storages and carbon sequestration potentials of the Grain for Green Program-Covered Forests in China. Ecol. Evol. 8, 7451–7461.
Xu, B., Guo, Z., Piao, S., Fang, J., 2010. Biomass carbon stocks in China's forests between 2000 and 2050: a prediction based on forest biomass-age relationships. Sci. China Life Sci. 53 (7), 776–783.
Yang, J., Dong, J., Xiao, X., Dai, J., Wu, C., Xia, J., Zhao, G., Zhao, M., Li, Z., Zhang, Y., Ge, Q., 2019. Divergent shifts in peak photosynthesis timing of temperate and alpine grasslands in China. Rem. Sens. Environ. 233.
Zhang, C., Ju, W., Chen, J.M., Zan, M., Li, D., Zhou, Y., Wang, X., 2013. China's forest biomass carbon sink based on seven inventories from 1973 to 2008. Clim. Chang. 118 (3–4), 933–948.
Zhang, C., Ju, W., Chen, J.M., Wang, X., Yang, L., Zheng, G., 2015. Disturbance-induced reduction of biomass carbon sinks of China's forests in recent years. Environ. Res. Lett. 10 (11).
Zhao, M., Yang, J., Zhao, N., Liu, Y., Wang, Y., Wilson, J.P., Yue, T., 2019. Estimation of China's forest stand biomass carbon sequestration based on the continuous biomass expansion factor model and seven forest inventories from 1977 to 2013. For. Ecol. Manag. 448, 528–534.